sciendo

DOI 10.2478/ama-2022-0028

acta mechanica et automatica, vol.16 no.3 (2022)

SIMULATION EVALUATION OF THE INFLUENCE OF SELECTED GEOMETRIC PARAMETERS ON THE OPERATION OF THE PNEUMATIC BRAKING SYSTEM OF A TRAILER WITH A DIFFERENTIAL VALVE

Dariusz SZPICA*, Marcin KISIEL*, Jarosław CZABAN*

*Faculty of Mechanical Engineering, Bialystok University of Technology,
ul. 45C Wiejska, 15-351 Bialystok, Poland

d.szpica@pb.edu.pl, m.kisiel@windowslive.com, j.czaban@pb.edu.pl

received 10 April 2022, revised 9 June 2022, accepted 10 June 2022

Abstract: This article presents simulation models of trailer air brake systems in configurations without a valve and with a differential valve, thus demonstrating the rationale for using a valve to improve system performance. Simplified mathematical models using the lumped method for systems without and with a differential valve are presented. The proposed valve can have two states of operation depending on the configuration of relevant parameters. These parameters can include the length of the control pipe, the throughput between chambers in the control part of the valve and the forcing rise time. Based on the calculations, it was found that the differential valve with large control pipe lengths can reduce the response time of the actuator by 42.77% relative to the system without the valve. In the case of transition of the valve to the tracking action, this time increases only by 9.93%. A force rise time of 0.5 s causes the transition of the valve from the accelerating action to the tracking action, with 9.23% delay relative to the system without a valve. The calculations can be used in the preliminary assessment of the speed of operation of pneumatic braking systems and in the formulation of guidelines for the construction of a prototypical differential valve. In conclusion, it is suggested to use a mechatronic system enabling smooth adjustment of the flow rate between chambers of the control system of the differential valve.

Key words: mechanical engineering, air braking system, differential valve, simulation

1. INTRODUCTION

Modern truck tractors, farm tractors and trains are equipped with air brake systems that control the performance of brakes in trailers, semi-trailers, farm machinery and railroad cars. The brake control units allow smooth operation of the braking system in a strictly predictable and controlled manner. This makes it possible to achieve the required braking efficiency and the response time of actuators (pneumatic actuators) in response to a stimulus such as pressing the brake pedal by the driver and the operation of the main brake control valve [1]. Pneumatic braking systems of vehicles are subjected to high requirements laid down in UNECE Regulation No. 13 [2]. Considering the increasing overall dimensions of vehicle assemblies with pneumatically actuated brakes and taking into account the larger distances between pressure tanks and actuators [3], it becomes necessary to apply an intermediate component whose purpose is to increase the rate of application of the trailer's brakes and to stabilise the supply pressure to the actuators of the braking system.

The intermediate elements in the pneumatic braking systems of towed assemblies are valves of various types. These may be relay valves [4–6] that use additional air tanks located close to actuators in the form of pneumatic actuators. The use of relay valves in the construction of the system makes it possible to shorten the system's response time to an excitation and to increase the braking force. These valves can only perform a specific function without the possibility of a free transition from a proportional action to an accelerating action depending on the nature of the excitation. Therefore, the concept of using differential valves has emerged [7–9]. The assumptions of the control theory state that a differential member in the control system influences the amplification of the output signal, which, when applied in a braking system, will positively influence the operation and response time of the system. The differential control systems operate in two ranges: in transient states, which occur in real control systems, they include an accelerating action, whereas in steady states, in which there are no changes in the output signal, the differential member maintains a tracking action [10]. There are also concepts of combination valves [11], purely pneumatic or electropneumatic [12].

The flow process is characterised by high complexity. It can be described by differential equations for the three-dimensional space using the Reynolds-averaged Navier–Stokes (RANS) method [13,14]. Dedicated software, such as KIVA, Ansys Fluent and others [15–18], is usually used to solve this problem. It is also possible, assuming certain simplifications, to reduce the space to a finite-dimensional and time-domain model of a physical system. The partial differential equations can be replaced by ordinary differential equations with a finite number of parameters. The discretisation process itself can indicate the possibility of describing the state in specific spaces, which are, for example, concentrated volumes.

Computer simulation makes it possible to graphically represent the time courses of pressure variations in the brake actuator chambers and to determine the characteristics of the pneumatic system components based on a mathematical model [19]. The realisation of the mathematical model is possible by discretizing the components, such as the lumped method [5,8,9].

Simulations using the lumped method can apply to relay valves [6], differential valves [9], or modified relay valves [1].

In a previous study [11], the differential equations formulated for various components of a dual brake valve (DBV), such as the main piston, main valve, relay piston and relay valve, were presented. The model was implemented in MATLAB/Simulink to capture the dynamic pressure characteristics of the DBV. Additionally, a mathematical model of the DBV was created in Amesim to verify the proposed approach.

The subject of a number of studies is the computational evaluation of the performance of an air braking system. Braking time delay is indicated as the main drawback of air braking systems, leading to dangerous driving situations resulting from insufficient system performance. In a previous study [12], the structure of a semitrailer tractor air brake system was optimised by adding a shuttle valve and a two-position, three-port solenoid valve between the control pipe and the charging pipe downstream of the semitrailer control valve. The simulation results showed significant improvements in braking time, stopping distance, longitudinal kinetic energy, transverse kinetic energy and phase plane. An experimental study [20] was concerned with a comprehensive evaluation of the performance of the electropneumatic braking system compared to that of the conventional pneumatic braking system. The experimental research indicated the advantage of the system with the electric part over the classic system. The efficiency of the systems, their costs and the degree of development were analysed.

In addition to road vehicles, simulations also apply to trains and railcars. In another study [21], different computer simulation scenarios were considered to study the effect of braking forces on the longitudinal dynamics of a train under different braking modes. A mathematical model of the pneumatic system and the control unit of the wagon was developed. In a study [22], fluid continuity and momentum equations were used to develop air flow equations. Using the finite element method, a braking model was obtained to account for the effect of air flow in long train pipes, as well as the effect of leakage and flow in branch pipes.

This study is an extension of another study [9], in which only the usefulness of using a differential valve in the pneumatic braking system of road trains was indicated. This study additionally includes a systematised model description along with precisely specified technical data and conditions necessary to initiate the simulation. Multivariate adjustments of the significant parameters of two braking systems, that is, without and with a differential valve, allowed to indicate the differences in the pressure courses in the selected volumes of the concentrated systems and to develop conclusions. Conclusions drawn from the analyses will allow for the evaluation of the feasibility of a differential valve in the trailer braking system. Additionally, an important issue remains whether it was necessary to use mechatronic systems which are capable of correcting, on an ongoing basis, the course of the braking process.

The structure of this article is as follows. The introduction to the mathematical modelling of the pneumatic braking systems is described in Section 2, followed by the structure of the analysed braking systems in Section 3 and their technical data and the conditions necessary to run the simulations in Section 4. The simulation results at variable transmission pipe lengths, throughputs between the chambers of the differential valve and control pressure rise times are described in Section 5. The last section presents the conclusions.

2. MATHEMATICAL MODELLING

The study uses the lumped method [8], which discretises a pneumatic system into basic members referred to as volume (V) and resistance (R). Combining the individual members V-R-V-…-R-V together allows the construction of pneumatic systems [4,23]. In developing the mathematical description of the basic components of the lumped method, the following simplifications were adopted:

- Air was treated as a thermodynamically ideal gas, being viscous and compressible.
- Isentropic flow in the adiabatic envelope took place without internal friction and without heat exchange with the surroundings.
- The state of the air was constant in each concentrated volume and depended only on time.
- The concentrated volumes were constant [8].
- The temperature during the process was constant [24].
- The connections of the individual system components were perfectly tight.
- Flow-restricting elements open and close gradually;
- The flow coefficient does not change during the transition process.

Fig. 1 shows a schematic diagram demonstrating the essence of discretisation of pneumatic system components in the lumped method.

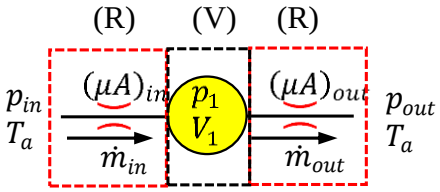

Fig. 1. Diagrams describing the equilibrium state of a concentrated volume (lumped method): p_{in}, p_1, p_{out} – absolute inlet, in concentrated volume, outlet pressure; T_a – absolute temperature of the air; V_1 – total volume in concentrated volume; $(\mu A)_{in}$ – inlet throughputs (conductance); $(\mu A)_{out}$ – outlet throughputs (conductance); $\dot{m}_{in}$ – inlet air mass flow; $\dot{m}_{out}$ – inlet air mass flow; (V) – volume; (R) - resistance

Based on Fig. 1, the pressure change in the concentrated volume (V) using mass flux balance is described by relation (1).

$$\frac{\mathrm{d}p_1}{\mathrm{d}t} = \frac{\kappa R_g T_a}{V_1}(\dot{m}_{in} - \dot{m}_{out}), \tag{1}$$

where κ =1.4 is adiabatic exponent and R_g = 287.05 J/(kg K) is the gas constant.

The air mass flow rate through the pneumatic drag was based on the Saint-Venant–Wantzel relation in the generalised form (Eqs (2) and (3)).

$$\dot{m}_{in} = (\mu A)_{in} \frac{p_{in}}{\sqrt{R_g T_a}} \psi_{\max} \psi(\sigma), \tag{2}$$

$$\dot{m}_{out} = (\mu A)_{out} \frac{p_1}{\sqrt{R_g T_a}} \psi_{\max} \psi(\sigma), \tag{3}$$

where $\psi_{\max}$ is the maximum value of the Saint-Venant–Wantzel function and $\psi(\sigma)$ is the dimensionless flow function.

sciendo
DOI 10.2478/ama-2022-0028

The maximum value of the Saint-Venant–Wantzel function for the critical pressure ratio σ^* = 0.528 [25] was calculated according to Eq. (4).

$$\psi = \sqrt{\left(\frac{2}{\kappa-1}\right)^{\frac{\kappa+1}{\kappa-1}}} = 0.578. \tag{4}$$

The dimensionless flow function was adopted according to Metlyuk–Avtushko [8] Eq. (5):

$$\psi(\sigma) = 1.13\frac{1-\sigma}{1.13-\sigma}, \tag{5}$$

where $\sigma = \frac{p_{aft}}{p_{bef}}$ and p_{bef} and p_{aft} are the pressures before and after resistance, respectively.

Substituting Eqs (2) and (3) into Eq. (1), we obtained a differential equation describing the pressure change in the concentrated volume according to Fig. 1 (Eq. (6)).

$$\frac{dp_1}{dt} = \frac{\kappa R_g T_a}{V_1}\left(\begin{matrix}(\mu A)_{in}\frac{p_{in}}{\sqrt{R_g T_a}}0.653\frac{p_{in}-p}{1.13p_{in}-p} - \\ +(\mu A)_{out}\frac{p}{\sqrt{R_g T_a}}0.653\frac{p-p_{out}}{1.13p-p_{out}}\end{matrix}\right). \tag{6}$$

This equation can be used to describe pressure changes in supply reservoirs and fixed chambers of valves, connections or actuators. Flow capacities (μA) determine the flow properties of pneumatic resistors such as nozzles, valves or connections. For pneumatic pipes, the cross-sectional area should be calculated from the pipe diameter, and the value of the flow coefficient should be determined from relation (7).

$$\mu = \frac{\mu_n}{\sqrt{n}}, \tag{7}$$

where μ_n = 0.12…0.28 (0.35) is the discharge coefficient of a 1-m-long pipe section and n is number of 1-m-length sections in the design pipe.

It has been suggested in a previous study [8] that the flow coefficient for pneumatic pipes can be discretised singularly to elements not exceeding 2.5 m in length. Therefore, this option was adopted in the simulation of this study.

In this way, it is possible to build pneumatic systems using a combination of members (V) and (R). Note that it is possible to connect several members (R) to one member (V).

3. ANALYSED SYSTEMS

Two air brake systems were adopted for comparative analysis: one without a differential valve (Fig. 2a) and the other with a differential valve (Fig. 2b). In the system without a differential valve, the air is accumulated in tank *1* at pressure $p_{\max}$ and supplied via pipe *2* to vehicle's brake valve *3*. At the moment when valve *3* is actuated (force F appears, which in this case will be represented as a function of p_{imp}), the air will begin to flow through valve *3* to pipe *4a* and further to actuator *5*. In the simulations, pipe *4a* will have different lengths. The concentrated volumes are constant and have been described as (p, V). In these volumes, the pressure waveforms can be read and analysed. In the system with a differential valve (Fig. 2b), the difference consists in shortening the length of pipe *4a* from Fig. 2a by 1 m, thus obtaining pipe *4b* (Fig. 2b) and supplementing the missing length with pipes *7* (0.2 m) and *10* (0.8 m).

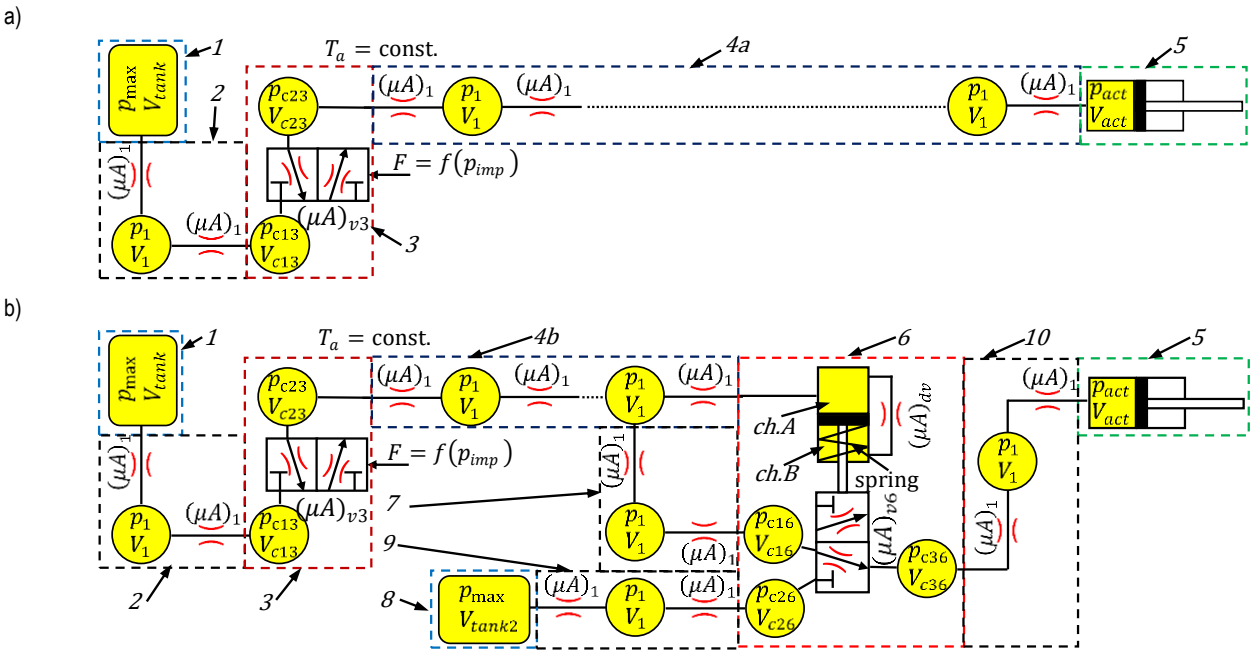

Fig. 2. Diagrams of the analysed braking systems: a – without a differential valve; b – with a differential valve; *1* and *8* – tank; *2*, *4*, *7*, *9* and *10* – pipes; *3* – vehicle brake valve; *6* – trailer differential brake valve; description in the text and Table 1

This is dictated by the use of differential valve *6*. Actuation of tractor control valve *3* causes the air to flow to pipes *4a* and *7*, which, in the initial stage of the differential valve operation, provides tracking action in the valve transmission part (valve bottom). Further air flows through pipe *10* to actuator *5*.

The transition from the tracking action of the differential valve to the accelerating action will occur when the pressure in *ch.A* overcomes the force from the spring and the valve transfer section is switched to supply from tank *8* and pipe *9*.

The accelerating action will occur until the increase in

pressure in *ch.B* combined with the force from the spring overcomes the pressure in *ch.A*. The acceleration action is mainly determined by the stiffness of the spring and the capacity between chambers *ch.A* and *ch.B,* defined as $(\mu A)_{dv}$. The values of these parameters determine the occurrence of the acceleration action and its duration. In the simulations, the spring stiffness will remain constant, while the throughput between chambers will undergo changes.

4. TECHNICAL DATA AND CONDITIONS NECESSARY TO INITIATE A SIMULATION

For the purpose of the simulation, it is necessary to assume the values of the technical parameters describing the components of the systems under study. Tab. 1 presents the technical parameters with a breakdown into elements according to Fig. 2. In defining the parameters and initial conditions, data provided in previous studies [5,9,29] were used. The underlined values indicate their variability within specified limits. Due to the comparative nature of the simulation, the volumes of the individual valve chambers and the unit capacities of the pipes were assumed to be the same. In accordance with a previous study [8], the pipes were unit discretised to elements not exceeding 2.5 m in length. The actuator represents a fixed volume resulting from half of its operating stroke.

To initiate the simulation, initial values must be specified in the components of the systems. Tab. 2 shows the initial conditions of the simulation.

Tab. 1. Technical data of system components adopted for calculations (designations according to Figs. 2a and b)

No.	Parameter and volume	
1	V = 40 × 10^{-3} m^3; T_a = 293.15 K	
2	d = 13 × 10^{-3} m; A = 1.327 × 10^{-4} m^2; μ_n = 0.2; l = 0.5 m; n = 1; V = 66.37 × 10^{-6} m^3; V_1 = 66.37 × 10^{-6} m^3; T_a = 293.15 K	
3	V_{c12} =V_{c23} = 50 × 10^{-6} m^3; $(\mu A)_{v3}$ = 5 × 10^{-4} m^2; T_a = 293.15 K	
4	d = 13 × 10^{-3} m; A = 1.327 × 10^{-4} m^2; μ_n = 0.2; T_a = 293.15 K	
	Fig. 1a – variants without a differential valve:	Fig. 1b – variants with a differential valve:
	(5m): l = 5 m; n = 2; V = 663.66 × 10^{-6} m^3; V_1 = 331.83 × 10^{-6} m^3	(5m): l = 4 m; n = 2; V = 530.93 × 10^{-6} m^3; V_1 = 256.45 × 10^{-6} m^3
	(10m): l = 10 m; n = 4; V = 1.3273 × 10^{-3} m^3; V_1 = 331.83 × 10^{-6} m^3	(10m): l = 9 m; n = 4; V = 1.1946 × 10^{-6} m^3; V_1 = 298.65 × 10^{-6} m^3
	(15m): l = 15 m; n = 6; V = 1.9910 × 10^{-3} m^3; V_1 = 331.83 × 10^{-6} m^3	(15m): l = 14 m; n = 6; V = 1.8583 × 10^{-6} m^3; V_1 = 309.71 × 10^{-6} m^3
	(20m): l = 20 m; n = 8; V = 2.6546 × 10^{-6} m^3; V_1 = 331.83 × 10^{-6} m^3	(20m): l = 19 m; n = 8; V = 2.5249 × 10^{-6} m^3; V_1 = 315.24 × 10^{-6} m^3
5	V = 850 × 10^{-6} m^3; T_a = 293.15 K	
6	$V_{ch.A}$ = $V_{ch.B}$ = V_{c16} =V_{c26} = V_{c36} = 50 × 10^{-6} m^3; $(\mu A)_{dv}$ = (3.5…12.5) × 10^{-7} m^2; $(\mu A)_{v6}$ = 7.5 × 10^{-4} m^2; T_a = 293.15 K; d_p = 65 × 10^{-3} m; d_{pt} = 10 × 10^{-3} m; k = 0.7× 10^5 N/m	
7	d = 13 × 10^{-3} m; A = 1.327 × 10^{-4} m^2; μ_n = 0.2; l = 0.2 m; n = 1; V = 26.55 × 10^{-6} m^3; V_1 = 26.55 × 10^{-6} m^3; T_a = 293.15 K	
8	V = 40 × 10^{-3} m^3; T_a = 293.15 K	
9	d = 13 × 10^{-3} m; A = 1.327 × 10^{-4} m^2; μ_n = 0.2; l = 1 m; n = 1; V = 132.73 × 10^{-6} m^3; V_1 = 132.73 × 10^{-6} m^3; T_a = 293.15 K	
10	d = 13 × 10^{-3} m; A = 1.327 × 10^{-4} m^2; μ_n = 0.2; l = 0.8 m; n = 1; V = 106.18 × 10^{-6} m^3; V_1 = 106.18 × 10^{-6} m^3; T_a = 293.15 K	

Glossary: d – pipe diameter; A – pipe cross-sectional area; μ_{ij} – pipe loss factor of a single section; l – pipe length; n – pipe number of components R-V; V – tank and pipe total volume; V_1 – pipe component volume; V_{c13}, V_{c23}, V_{c16}, V_{c26}, V_{c36}, $V_{ch.A}$ and $V_{ch.B}$ – chamber volume; V_{tank} and V_{tank2} – actuator volume; T_a – air temperature; d_p – valve piston diameter; d_{pt} – valve piston rod diameter; k – spring stiffness.

Tab. 2. Initial conditions at t = 0 s (according to Fig. 2)

Parameter	Value
Pressure in tank *1* and *8*, pipe *2* and *9*, chamber V_{c13} and V_{c26}	8 × 10^5 Pa
Pressure in pipe *4a* / *4b*, *7* and *10*, chamber V_{c23}, V_{c16}, V_{c36}; $V_{ch.A}$, $V_{ch.B}$, actuator V_{act}	1 × 10^5 Pa
Pressure of the forcing pulse p_{imp} in valve *3*	1 × 10^5 Pa
Setting valves *3* and *6*	As shown in Fig. 2

The pressure change in each focused volume according to Fig. 2 was created according to Eq. (6). Due to the extensiveness of the description, it will not be presented in the article.

In both analysed systems (without and with a differential valve) at the start of the simulation, valve *3* (Figs. 2a and b) opens according to the assumed rising time of the control pressure to the maximum value. The rising time is described by t_{tfp}, whose value characterises the braking mode – rapid or slow. The change in control pressure is given in the following Eq. (8):

$$\frac{\mathrm{d}p_{imp}}{\mathrm{d}t} = (p_{\max} - p_a)\frac{t}{t_{tfp}} + p_a \text{ for } 0 \le t < t_{tfp}. \quad (8)$$

A change in pressure p_{imp} will result in a proportional change in the throughput $(\mu A)_{v3}$ and a gradual opening of valve *3* (Fig. 2).

In a system with a differential valve (Fig. 2b), the throughput in the transferring part (at the bottom of valve *6*) defined as $(\mu A)_{v6}$ will depend on the arrangement of forces in the control part (at the top of the valve). Depending on the overdrive of the transfer part, actuator *5* will be able to be supplied from pipes *4* and *7* (tracking action) or from tank *8* and pipe *9* (accelerating action).

The tracking action of valve *6* will occur when, in the control part, the force system has the following form (9):

$$p_{ch.A}F_{pch.A}\eta \le p_{ch.B}F_{pch.B}\eta + F_s. \quad (9)$$

Then the bandwidth in the transferring part will reach the maximum value, and the power will come from wire *7* according to Eq. (10).

$$(\mu A)_{v6} = (\mu A)_{v6\max} \text{ and } p = p_{c16}. \quad (10)$$

With the accelerating action of valve *6* in the control section, the force system will be of the following form (11):

$$p_{ch.A}F_{pch.A}\eta > p_{ch.B}F_{pch.B}\eta + F_s. \quad (11)$$

The throughput in the transfer section will also reach the maximum value, but the supply will come from tank *8* and pipe *9* according to Eq. (12).

$$(\mu A)_{v6} = (\mu A)_{v6\max} \text{ and } p = p_{c26}, \quad (12)$$

where $F_{ch.A}$ is the cross-sectional area of piston from chamber *A*; $F_{ch.A}$ is the cross-sectional area of the piston from chamber *ch.B*; η =0.95 is the coefficient of friction forces in the differential valve; F_s is the force from spring; and p is the input pressure in valve *6*.

The instantaneous difference in pressure values $p_{ch.A}$ and $p_{ch.B}$ is responsible for the throughput between these chambers $(\mu A)_{dv}$. This mainly determines the occurrence or absence of the acceleration effect.

5. RESULTS OF THE SIMULATION

The differential equations describing the pressure changes in each control volume based on Eq. (6) were solved numerically by using the implicit trapezoid method combined with backward differentiation (min. step 1 × 10-6 s) in MATLAB/Simulink software [26]. This software is characterised by the ease of implementation of the adopted empirical models and the possibility of replicating the repeating subsytems using masking, as confirmed in studies [27–29].

The use of the differential valve should be assumed to reduce the operation time of the pneumatic system in the vehicle brake valve actuation – actuator relationship. In the initial part, two systems were simulated: one without a differential valve and the other with a differential valve. According to Tab. 1, the variant (20 m) was assumed and the throughput $(\mu A)_{dv}$ = 3.5 × 10-7 m2. Assuming an increase in the control pressure p_{imp} during 0.2 s to the maximum value, the pressure waveforms in the selected control volumes were obtained.

The system (20 m) without a differential valve is able to reach a pressure of 0.75 $p_{\max}$ in the control volume of the actuator in 1.218 s (Fig. 3).

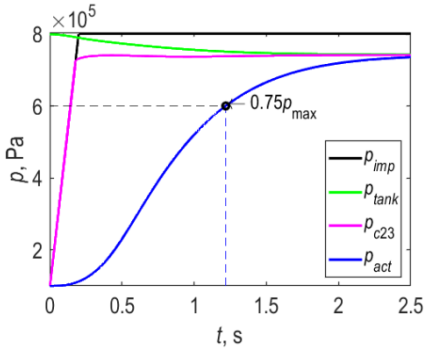

Fig. 3. Pressure curves in selected control volumes for the system without a differential valve and for the pipe length variant (20 m) at a control pressure rise time of 0.2 s; indexes: imp – control impulse; *tank* – tank, *c23* – chamber 23; *act* – actuator

By contrast, the system (20 m) with the differential valve achieves this pressure in 0.697 s (Fig. 4). The use of the differential valve resulted in a 42.77% reduction response time. The pressure waveform in the actuator control volume p_{act} (Fig. 4) shows the essence of the use of the differential valve. Up to point *A*, the system with the differential valve exhibits a tracking action, and a slight delay in this range relative to the system without a valve (Fig. 5) is due to the flow through the transfer system of the differential valve. At point *A* (Fig. 4), the pressure in the chamber *ch.A* of the control portion of the differential valve overcomes the force from the spring (Fig. 2) and, as a result, overrides the supply from tank *8*.

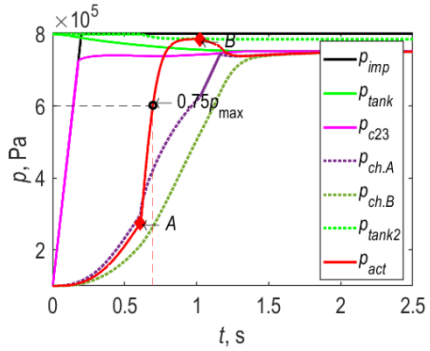

Fig. 4. Pressure curves in selected control volumes for the system with a differential valve and for the pipe length variant (20 m) at a control pressure rise time of 0.2 s and throughput $(\mu A)_{dv}$ 3.5 × 10-7 m2; indexes: *imp* – control impulse; *tank* and *tank2* – tank, *c23*, *ch.A* and *ch.B* – chamber 23; *act* – actuator; p. *A* – opening of the valve; p. *B* – closing of the differential valve

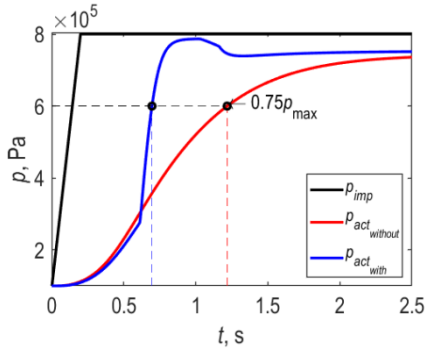

Fig. 5. Pressure curves in selected control volumes for the system without and with a differential valve and for the pipe length variant (20 m) at a control pressure rise time of 0.2 s and throughput $(\mu A)_{dv}$ 3.5 × 10-7 m2; indexes: *imp* – control impulse; *act* – actuator

The action ceases to be tracked, and because of the proximity of tank *8*, the pressure in the actuator p_{act} increases rapidly until it equals the pressure p_{tank2} (Fig. 4). The throughput $(\mu A)_{dv}$ allows the pressures in the chambers *ch.A* and *ch.B* to equalise and, by the additional action of the spring force, return to the tracking action (point *B*). Furthermore, the pressure in the actuator will tend to equalise with the pressure p_{tank}. The mode of operation of the combined chambers *ch.A* and *ch.B* (Fig. 2) in the differential valve differs from that in the relay valve [4,6].

Next, simulations were performed for all variants of wire length *4* and throughputs $(\mu A)_{dv}$ included in Tab. 1. The throughputs $(\mu A)_{dv}$ were graded in steps of 0.5 × 10-7 m2. As before, the control pressure increment p_{imp} was assumed at 0.2 s to a maximum value.

Calculations showed that for $(\mu A)_{dv}$ throughputs of (4.0, 5.0, 7.5 and 12.5) × 10-7 m2, respectively, successive variants of 4 (20,

15, 10 and 5) m pipe length cease to show an accelerating effect in the variant with the differential valve (Tab. 3 and Fig. 6). At $(\mu A)_{dv}$ = 3.5 × 10^{-7} m^2, all length variants exhibit an accelerating effect with respect to the system without the differential valve.

Tab. 3. Comparison of the times for reaching 0.75 $p_{\max}$ at different lengths of pipe *4* (Fig. 2)

Variant pipe length (m)	Without valve (s)	With differential valve (s) at throughput $(\mu A)_{dv}$ × 10^{-7} m^2								
		3.5	**4.0**	**4.5**	**5.0**	**5.5**	**6.0**	**6.5**	**7.0**	**7.5**
5	0.360	0.230	0.232	0.235	0.237	0.239	0.242	0.244	0.246	0.250
10	0.596	0.342	0.347	0.354	0.363	0.370	0.379	0.394	0.414	0.676
15	0.880	0.482	0.501	0.526	0.986	0.979	0.989	0.988	0.987	0.978
20	1.218	0.697	1.339	1.337	1.342	1.338	1.337	1.338	1.348	1.337
Variant pipe length (m)	**With differential valve (s) at throughput $(\mu A)_{dv}$ × 10^{-7} m^2**									
	8.0	**8.5**	**9.0**	**9.5**	**10.0**	**10.5**	**11.0**	**11.5**	**12.0**	**12.5**
5	0.252	0.255	0.259	0.263	0.267	0.272	0.275	0.282	0.295	0.410
10	0.677	0.675	0.677	0.674	0.676	0.672	0.672	0.678	0.672	0.678
15	0.979	0.988	0.982	0.988	0.981	0.987	0.983	0.977	0.978	0.984
20	1.338	1.339	1.346	1.343	1.334	1.343	1.335	1.338	1.340	1.339

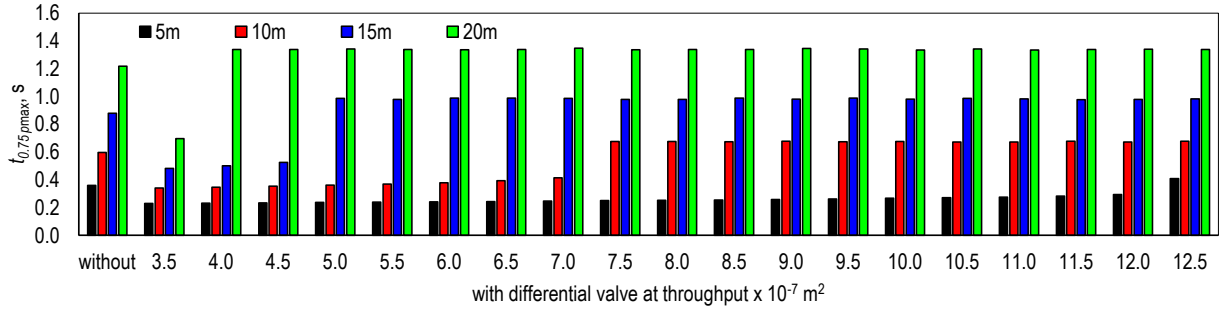

Fig. 6. Values of the times for reaching 0.75 $p_{\max}$ at different lengths of pipe *4* (Fig. 2)

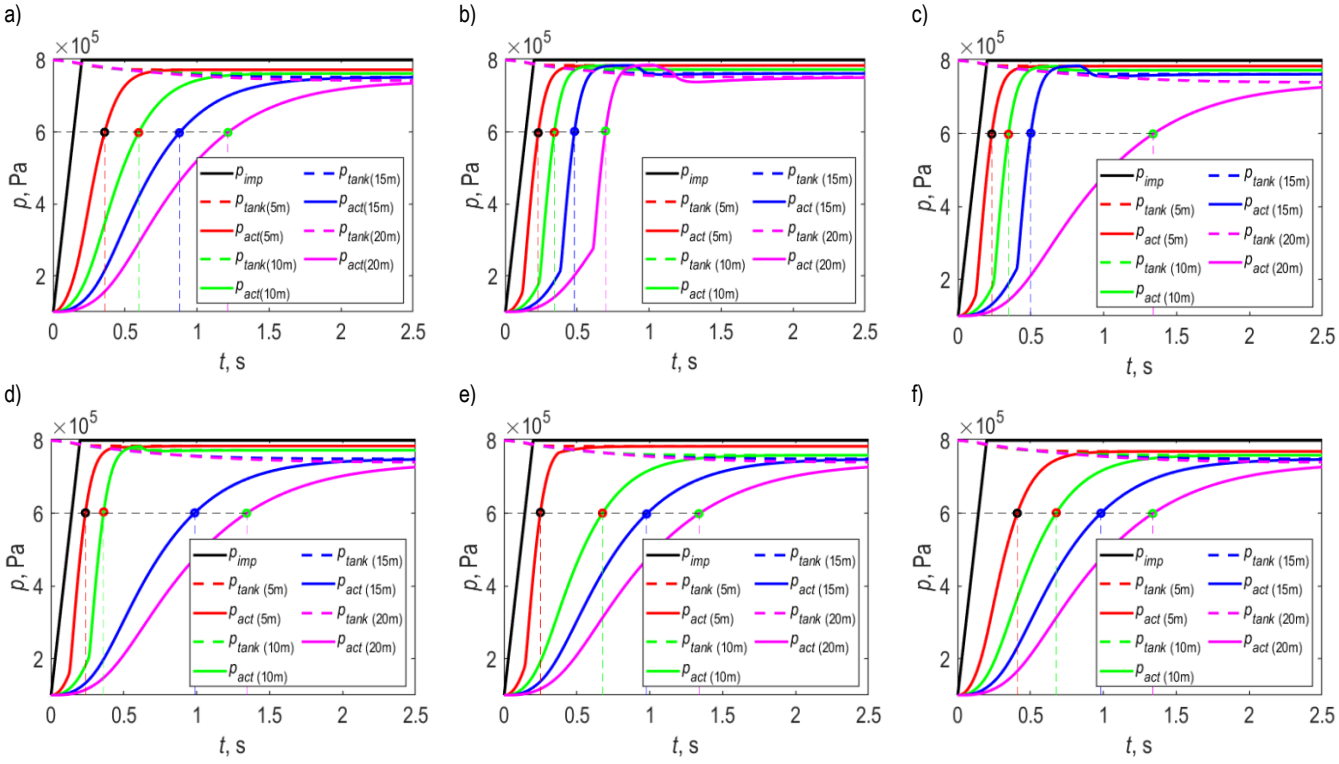

Fig. 7. Pressure curves in selected control volumes at a control pressure rise time of 0.2 s and at different lengths of pipe *4* (according to Tab. 1): (a) system without a differential valve, (b–f) system with a differential valve at throughputs $(\mu A)_{dv}$ × 10^{-7} m^2: b - 3. 5; c - 4; d - 5; e - 7.5; f - 12.5; indexes: *imp* – control impulse; *tank* – tank, *act* – actuator; (5, ..., 20) m – pipe length variants

In order to graphically represent the disappearance of the accelerating action of the differential valve, Fig. 7 shows the pressure waveforms in selected control volumes of the tested systems without and with the valve. For the differential valve, the throughputs $(\mu A)_{dv}$ were (3.5, 4.0, 5.0, 7.5 and 12.5) × 10^{-7} m^2, control pipe lengths 4 (5, 10, 15 and 20) m, respectively.

Taking the throughput step $(\mu A)_{dv}$ preceding the decay of the accelerating action of the differential valve as a reference point, differences in the reduction of the actuator response time were found between the variants.

In the variant of pipe length *4* (20 m) and throughput $(\mu A)_{dv}$ = 3.5 × 10^{-7} m^2, the differential valve caused a 42.77% reduction in the time to reach a pressure of 0.75 $p_{\max}$ in the actuator control volume. The variant (15 m) and $(\mu A)_{dv}$ = 4.5 × 10^{-7} m^2 reduced this time by 40.23%. By contrast, the variant (10 m) and $(\mu A)_{dv}$ = 7 × 10^{-7} m^2 showed a time reduction of 30.54%. The variant with the shortest wire length of 4 (5 m) and $(\mu A)_{dv}$ = 12 × 10^{-7} m^2 showed the least reduction in response time of 18.01%.

This demonstrated the validity of the use of differential valves in braking systems with large lengths of control pipe *4* (Fig. 2), as mentioned in the literature [1,8,9].

At the points of deceleration and tracking action, deceleration in the indicated cases was 13.89, 13.42, 12.04 and 9.93%, respectively, with the lowest value recorded for the variant with the longest pipe *4*.

In the last stage of the simulation, the effect of the control pressure rise time (p_{imp}) to the maximum value on the actuator response time was evaluated. The differential valve should guarantee its acceleration action at short override times of the vehicle brake valve. Such a situation replicates sudden braking, and then there is a need to brake the trailer as quickly as possible to prevent the trailer from "dropping" behind the towing vehicle [2,30].

For the analysis, systems without and with a differential valve in the variant (20 m) with a capacity of $(\mu A)_{dv}$ = 3.5 × 10^{-7} m^2 were adopted. The times of control pressure rise p_{imp} to a maximum value were taken as 0.2, 0.3, 0.4 and 0.5 s.

Comparing the times t_{tfp} necessary to reach 0.75 $p_{\max}$ in the control volume of the actuator (Tab. 4, Fig. 8), it is shown that the tracking action of the system with the differential valve is achieved at t_{tfo} = 0.5 s, where the actuator response time increases by 9.23% relative to the system without the differential valve.

Tab. 4. Comparison of the times for reaching 0.75 $p_{\max}$ at different control pressure rise times

Variant	Time to full pressure t_{tfp}, s			
	0.2	0.3	0.4	0.5
Without a differential valve	1.218	1.255	1.293	1.331
With a differential valve	0.697	0.756	0.841	1.454

Below this value, an accelerating effect becomes apparent. At t_{tfo} = 0.2 s, the system with an acceleration valve reduces the response time of the actuator by 42.77%. On the other hand, at t_{tfo} = 0.3 s, the time reduction is slightly smaller at 39.77%. In the next case, at t_{tfo} = 0.4 s, the reduction is 34.99%.

The differences in the times to reach 0.75 $p_{\max}$ in the control volume of the actuator (Fig. 9) are due to the time that must elapse before the transfer section of the differential valve is switched to supply from tank *8* (Fig. 2). This shows the increasingly later switching of the differential valve depending on the value of t_{tfo}.

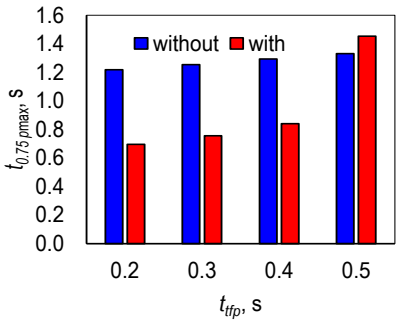

Fig. 8. Values of the times for reaching 0.75 $p_{\max}$ at different control pressure rise times

In this way, the possibility of a smooth transition of the system with the differential valve from an accelerating action to a tracking action with a small delay in relation to the system without the differential valve is demonstrated.

The choice of conductor parameters and the volume of the concentrated chambers of the analysed system allows to approximate the tracking performance of the system with a differential valve to the system without a valve. An important feature is the throughput $(\mu A)_{dv}$ and its influence on the valve performance when confronted with time t_{tfo}.

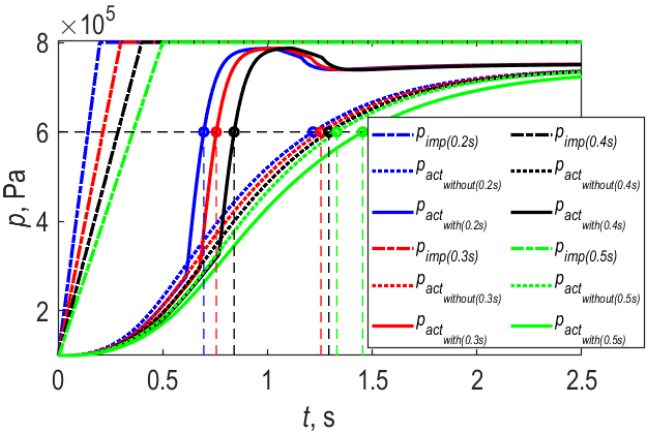

Fig. 9. Pressure curves in selected control volumes for the systems without and with a differential valve for the pipe length variant (20 m) at different control pressure rise times and throughput $(\mu A)_{dv}$ 3.5 × 10^{-7} m^2: a - t_{tfp} = 0.2 s; b - t_{tfp} = 0.3 s; a - t_{tfp} = 0.4 s; a - t_{tfp} = 0.5 s; indexes: *imp* - control impulse; *act* – actuator

It should be emphasised that the mathematical model presented in the article is simplified. It does not include a description of the variable volume of the control or actuator chambers and heat transfer. However, as can be judged from the simulation results obtained, it is useful for preliminary estimation of differences in the nature of operation of systems without and with a differential valve. The parameter that is considered important in the course of design and practical implementation of the differential valve is the throughput between the control chambers *ch.A* and *ch.B* defined as $(\mu A)_{dv}$ (Fig. 2). In

calculations, the value of the throughput was assumed constant in the considered variants and configurations of the system. After the simulations, it was found that designing a system enabling smooth regulation of this throughput via a mechatronic system is worth considering.

In the next steps, further work is planned to complete the mathematical model with variable volume chambers and heat transfer. The simulations performed and the analysis of their results are a prelude to the development of a prototypical differential valve. The design of a system enabling smooth adjustment of the flow rate between the valve chambers via a mechatronic system is also considered. In addition to the commonly used valves with electromagnetic actuation [31,32], piezoelectric actuation [33,34] is a certain hope.

The braking system is one of the components of the whole trailer. Considering broader possibilities of using the mathematical model presented in this article, there is a chance to use it to model the movement of a trailer or a tractor–trailer combination similar to the one presented in a previous study [35]. Additionally, the braking system model can be combined with other component models such as shock absorbers, springs, control arms or wheels, to evaluate vehicle handling. By supplementing the model presented in a pervious study [36] with the braking system, one can obtain a model of the entire trailer or tractor–trailer combination.

6. CONCLUSIONS

The simulations presented in the article were intended to demonstrate the purpose of using the differential valve in trailer braking systems. The proposed mathematical model, in spite of its simplifications, turned out to be useful for the preliminary comparative evaluation of the systems adopted without and with a differential valve. Based on the analyses performed, the following conclusions were reached.

1. The application of the differential valve in the braking system in all analysed variants of the control pipe length can result in the reduction of the actuator response time. In the case of a pipe with a length of 20 m and a throughput between the valve chambers of 3.5×10^{-7} m^2, the response time is reduced by 42.77%.
2. The dominant parameter affecting the performance of the differential valve is the throughput between its chambers. The throughput can reduce the response time or, depending on the value, change the valve action from accelerating to tracking. A system with a wire of 20 m length and a 4×10^{-7} m^2 throughput between chambers increases the response time by 9.93% while maintaining the tracking action.
3. The acceleration effect of the differential valve system depends on the course of the forcing pulse. For the rise times of the control pressure to the maximum value below 0.5 s, the acceleration effect was obtained (the maximum at 0.2 s was by 42.77%). At a rise time of 0.5 s, the action changed to tracking with 9.23% retardation with respect to the system without a valve.
4. Based on the calculations and analyses performed, it is suggested that a mechatronic system could be used to enable smooth adjustment of the flow rate between the chambers of the differential valve control system. This type of system could adjust the differential valve to the characteristics of the trailer.

REFERENCES

1. Kamiński Z, Kulikowski K. Determination of the functional and service characteristics of the pneumatic system of an agricultural tractor with mechanical brakes using simulation methods. Eksploatacja i Niezawodność - Maintenance and Reliability. 2015;17(3):355–64.
2. Regulation No 13 of the Economic Commission for Europe of the United Nations (UN/ECE) — Uniform provisions concerning the approval of vehicles of categories M, N and O with regard to braking [Internet]. Official Journal of the European Union. 2015 [cited 2022 Apr 3]. Available from: http://data.europa.eu/eli/reg/2016/194/oj
3. Krichel S V, Sawodny O. Dynamic modeling of pneumatic transmission lines in Matlab/Simulink. In: International Conference on Fluid Power and Mechatronics - 17-20 Aug 2011, Beijing, China. Beijing, China: IEEE; 2011. p. 24–9.
4. Kulesza Z, Siemieniako F, Mikołajczyk B. Modelowanie zaworu przekaźnikowo-sterującego. Pneumatyka. 2008;1:31–5.
5. Kamiński Z. Mathematical modelling of the trailer brake control valve for simulation of the air brake system of farm tractors equipped with hydraulically actuated brakes. Eksploatacja i Niezawodność - Maintenance and Reliability. 2014;16(4):637–43.
6. Kulesza Z, Siemieniako F. Modeling the air brake system equipped with the brake and relay valves. Zeszyty Naukowe. 2010;24(96): 5–11.
7. Beater P. Pneumatic Drives. System Design, Modelling and Control. Springer; 2007.
8. Miatluk M, Avtuszko F. Dinamika pnievmaticeskich i gidravliceskich privodov avtomobilej. M. Maszinostrojenije; 1980. 231 p.
9. Szpica D. Modeling of the operation of a pneumatic differential valve increasing the efficiency of pneumatic brake actuation of road trains. In: Transport Means - Proceedings of the International Conference. 2018. p. 151–6.
10. Mystkowski A. Zastosowanie zaworów różniczkujących w pneumatycznych układach napędowych. Pneumatyka. 2004;3:21–3.
11. Patil JN, Palanivelu S, Jindal AK. Mathematical model of dual brake valve for dynamic characterization. In: SAE Technical Papers. SAE International; 2013.
12. Jing Z, He R. Electronic structural improvement and experimental verification of a tractor-semitrailer air brake system. Proceedings of the Institution of Mechanical Engineers, Part D: Journal of Automobile Engineering. 2020 Jul 1;234(8):2154–61.
13. Yang Z, Cheng X, Zheng X, Chen H. Reynolds-Averaged Navier-Stokes Equations Describing Turbulent Flow and Heat Transfer Behavior for Supercritical Fluid. Journal of Thermal Science. 2021;30(1).
14. Matyushenko AA, Garbaruk A V. Adjustment of the k-ω SST turbulence model for prediction of airfoil characteristics near stall. In: Journal of Physics: Conference Series. 2016.
15. Yu W, Yang W, Zhao F. Investigation of internal nozzle flow, spray and combustion characteristics fueled with diesel, gasoline and wide distillation fuel (WDF) based on a piezoelectric injector and a direct injection compression ignition engine. Applied Thermal Engineering. 2017;114.
16. Michalcová V, Kotrasová K. The numerical diffusion effect on the cfd simulation accuracy of velocity and temperature field for the application of sustainable architecture methodology. Sustainability (Switzerland). 2020;12(23):10173.
17. Cvetkovic D, Cosic I, Subic A. Improved performance of the electromagnetic fuel injector solenoid actuator using a modelling approach. International Journal of Applied Electromagnetics and Mechanics. 2008;
18. Szpica D, Mieczkowski G, Borawski A, Leisis V, Diliunas S, Pilkaite T. The computational fluid dynamics (CFD) analysis of the pressure sensor used in pulse-operated low-pressure gas-phase solenoid valve measurements. Sensors. 2021;21(24):8287.
19. Subramanian SC, Darbha S, Rajagopal KR. Modeling the pneumatic subsystem of an s-cam air brake system. Journal of Dynamic Systems, Measurement and Control, Transactions of the ASME.

2004;126(1):36–46.
20. Kumar EA, Gautam V, Subramanian SC. Performance evaluation of an electro-pneumatic braking system for commercial vehicles. In: ICPCES 2012 - 2012 2nd International Conference on Power, Control and Embedded Systems. 2012.
21. Afshari A, Specchia S, Shabana AA, Caldwell N. A train air brake force model: Car control unit and numerical results. Proceedings of the Institution of Mechanical Engineers, Part F: Journal of Rail and Rapid Transit. 2013;227(1):38–55.
22. Aboubakr AK, Volpi M, Shabana AA, Cheli F, Melzi S. Implementation of electronically controlled pneumatic brake formulation in longitudinal train dynamics algorithms. Proceedings of the Institution of Mechanical Engineers, Part K: Journal of Multi-body Dynamics. 2016;230(4):505–26.
23. Kamiński Z. A simplified lumped parameter model for pneumatic tubes. Mathematical and Computer Modelling of Dynamical Systems. 2017;23(5):523–35.
24. Iwaszko J. Wymiana ciepła podczas opróżniania zbiornika. Zeszyty Naukowe Politechniki Łódzkiej, Cieplne Maszyny Przepływowe. 1988;93:12–21.
25. Grymek S, Kiczkowiak T. Conversion of the sonic conductance C and the critical pressure ratio b into the airflow coefficient μ. Journal of Mechanical Science and Technology. 2005;19(9):1706–10.
26. Yang WY, Cao W, Chung T-S, Morris J. Applied Numerical Methods Using MATLAB®. Applied Numerical Methods Using MATLAB®. Wiley & Sons; 2020. 1–502 p.
27. Shamdani AH, Shameki AH, Basharhagh MZ, Aghanajafi S. Modeling and simulation of a diesel engine common rail injector in Matlab/Simulink. In: 14 th Annual (International) Mechanical Engineering Conference – May 2006 Isfahan University of Technology, Isfahan, Iran. 2006. p. 7.
28. Demarchi A, Farçoni L, Pinto A, Lang R, Romero R, Silva I. Modelling a solenoid's valve movement. In: Lecture Notes in Computer Science (including subseries Lecture Notes in Artificial Intelligence and Lecture Notes in Bioinformatics). 2018.
29. Kamiński Z. Experimental and numerical studies of mechanical subsystem for simulation of agricultural trailer air braking systems. International Journal of Heavy Vehicle Systems. 2013;20(4):289–311.
30. Czaban J, Kamiński Z. Diagnosing of the agricultural tractor braking system within approval tests. Eksploatacja i Niezawodność - Maintenance and Reliability. 2012;14(4):319–26.
31. Hung NB, Lim O, Yoon S. Effects of Structural Parameters on Operating Characteristics of a Solenoid Injector. In: Energy Procedia. 2017. p. 1771 – 1775.
32. Plavec E, Ladisic I, Vidovic M. The impact of coil winding angle on the force of DC solenoid electromagnetic actuator. Advances in Electrical and Electronic Engineering. 2019;17(3):244–50.
33. Mieczkowski G, Szpica D, Borawski A, Diliunas S, Pilkaite T, Leisis V. Application of smart materials in the actuation system of a gas injector. Materials. 2021;14(22):6984.
34. Mieczkowski G. Static electromechanical characteristics of piezoelectric converters with various thickness and length of piezoelectric layers. Acta Mechanica et Automatica. 2019;13(1):30–6.
35. Liu Y. Modeling abstractions of vehicle suspension systems supporting the rigid body analysis. International Journal of Vehicle Structures and Systems. 2010;2(3–4):117–26.
36. Liu Y. Constructing equations of motion for a vehicle rigid body model. SAE International Journal of Passenger Cars - Electronic and Electrical Systems. 2009;1(1):1289–97.

This research was financed through subsidy of the Ministry of Science and Higher Education of Poland for the discipline of mechanical engineering at the Faculty of Mechanical Engineering Bialystok University of Technology WZ/WM-IIM/4/2020.

Dariusz Szpica: https://orcid.org/0000-0002-7813-8291

Marcin Kisiel: https://orcid.org/0000-0002-4576-0447

Jarosław Czaban: https://orcid.org/0000-0002-0677-7342